European Heart Journal (2005) **26**, 2320–2324
doi:10.1093/eurheartj/ehi357

Reproducibility of 3D free-breathing magnetic resonance coronary vessel wall imaging

Milind Y. Desai[1,2,5], Shenghan Lai[3], Christoph Barmet[6], Robert G. Weiss[2], and Matthias Stuber[1,2,4]*

[1] *Russell. H. Morgan Department of Radiology and Radiologic Sciences, Johns Hopkins University Medical School, JHOC 4243, 601, North Caroline Street, Baltimore, MD 21287, USA;* [2] *Department of Medicine, Johns Hopkins University Medical School, JHOC 4243, 601, North Caroline Street, Baltimore, MD 21287, USA;* [3] *Department of Pathology, Johns Hopkins University Medical School, JHOC 4243, 601, North Caroline Street, Baltimore, MD 21287, USA;* [4] *Department of Electrical Engineering, Johns Hopkins University Medical School, JHOC 4243, 601, North Caroline Street, Baltimore, MD 21287, USA;* [5] *National Institutes of Health, Bethesda, MD, USA; and* [6] *Institute of Biomedical Engineering, University and ETH, Zurich, Switzerland*

Received 24 January 2005; revised 2 May 2005; accepted 10 May 2005; online publish-ahead-of-print 21 June 2005

KEYWORDS
Coronary artery vessel wall imaging;
Magnetic resonance imaging;
Reproducibility

Aims Although the coronary artery vessel wall can be imaged non-invasively using magnetic resonance imaging (MRI), the *in vivo* reproducibility of wall thickness measures has not been previously investigated. Using a refined magnetization preparation scheme, we sought to assess the reproducibility of three-dimensional (3D) free-breathing black-blood coronary MRI *in vivo*.
Methods and results MRI vessel wall scans parallel to the right coronary artery (RCA) were obtained in 18 healthy individuals (age range 25–43, six women), with no known history of coronary artery disease, using a 3D dual-inversion navigator-gated black-blood spiral imaging sequence. Vessel wall scans were repeated 1 month later in eight subjects. The visible vessel wall segment and the wall thickness were quantitatively assessed using a semi-automatic tool and the intra-observer, inter-observer, and inter-scan reproducibilities were determined. The average imaged length of the RCA vessel wall was 44.5 ± 7 mm. The average wall thickness was 1.6 ± 0.2 mm. There was a highly significant intra-observer ($r = 0.97$), inter-observer ($r = 0.94$), and inter-scan ($r = 0.90$) correlation for wall thickness (all $P < 0.001$). There was also a significant agreement for intra-observer, inter-observer, and inter-scan measurements on Bland–Altman analysis. The intra-class correlation coefficients for intra-observer ($r = 0.97$), inter-observer ($r = 0.92$), and inter-scan ($r = 0.86$) analyses were also excellent.
Conclusion The use of black-blood free-breathing 3D MRI in conjunction with semi-automated analysis software allows for reproducible measurements of right coronary arterial vessel-wall thickness. This technique may be well-suited for non-invasive longitudinal studies of coronary atherosclerosis.

Introduction

With the recognition that the process of coronary atherosclerosis involves progressive arterial remodelling,[1] the focus of cardiovascular imaging is shifting from the arterial lumen to the vessel wall. Non-invasive imaging approaches that assess coronary wall characteristics accurately and reproducibly offer the promise of detecting coronary atherosclerosis before it manifests clinically. In the coronary arterial tree, this can be achieved non-invasively by measuring the calcium burden in the vessel wall using electron beam computed tomography[2] or invasively by intra-vascular ultrasound (IVUS).[3]

Magnetic resonance imaging (MRI), because of its truly non-invasive nature and excellent soft-tissue contrast, has been investigated as a modality to image atherosclerotic abnormalities in the coronary vessel wall.[4] The first description demonstrated that the coronary wall thickness could be measured with black-blood, fat suppressed MRI, and coronary arterial wall remodelling could be visualized.[4] However, in the original description, the visualization of the coronary vessel wall was limited by reduced coverage [because of two-dimensional (2D)imaging] and constraints related to repeated breath-holds. Botnar *et al*. attempted to overcome these shortcomings by imaging the right coronary wall using three-dimensional (3D), free-breathing black-blood coronary MRI.[5,6] Using that method, arterial remodelling was successfully identified in a patient cohort with X-ray defined non-significant coronary artery disease.[5] That approach used an innovative 2D local dual inversion pre-pulse to generate contrast between the vessel wall and the coronary lumen. However, to the best of our knowledge, the reproducibility of this technique has not been ascertained. In this study, we sought to evaluate the inter-scan, inter- and intra-observer reproducibilities of vessel wall thickness of the right coronary artery (RCA) in healthy adult subjects, using 3D free-breathing black-blood coronary MRI.

* Corresponding author. Tel: +1 443 287 5241; Fax: +1 410 614 1977.
E-mail address: mstuber@mri.jhu.edu

Methods

This study was conducted at Johns Hopkins Medical Institutions after obtaining appropriate institutional review board approval and informed consent from each participant. The study participants consisted of consecutively enroled 18 healthy individuals (age range 25–43), with no prior history of cardiovascular disease and who responded to flyers posted in the hospital. All the subjects were in sinus rhythm, without contraindications to MRI. The study was repeated $\sim$1 month later in eight subjects to assess inter-scan reproducibility.

MRI technique

All the MR scans were performed on a commercial 1.5 T system (Gyroscan Intera, Phillips Medical Systems, Best, The Netherlands) equipped with PowerTrak 6000 gradients (23 mT/m, 219 μs rise time). The subjects were imaged in the supine position using a five-element cardiac phased-array receiver coil, vector ECG triggering,[7] and arrhythmia rejection software. All scans were obtained using un-coached free-breathing and both the angiogram and the vessel wall scans were performed with a right hemi-diaphragmatic 2D selective navigator with a 5 mm gating window applied in the foot–head direction for respiratory motion suppression. To further constrain residual respiratory motion within that 5 mm gating window, real-time prospective adaptive slice-following[8] with a superior–inferior correction factor of 0.6[9] accounting for the motion of the RCA relative to the diaphragm was utilized.

Coronary artery localization and angiography

A free-breathing, navigator-gated, and corrected axial scan was obtained for the identification of the RCA. On these images, accurate volume targeting in parallel to the RCA was obtained using a three-point plan scan tool, applied at three different anatomic levels (proximal, mid, and distal).[10] Subsequently, a retrospectively triggered functional steady state with free precession (SSFP) scan ($\alpha = 75^\circ$, TR = 2.8 ms, and TE = 1.4 ms) with a high temporal resolution of 20 ms was obtained to identify the period of least cardiac motion. On the images of this scan, the period of minimal RCA displacement was visually identified and the time delay between the R-wave of the ECG and this period of minimal myocardial motion (Td) was recorded. All subsequent high-resolution images were obtained at that Td. In order to visualize the RCA lumen and to aid in accurate localization of the area of maximized contrast enhancement for subsequent vessel wall scanning, a double oblique navigator-gated and corrected 3D bright blood coronary MR angiogram (SSFP sequence with a T2 preparation pulse) was then obtained (TR = 5.8, TE = 2.9, flip angle = 70°, FOV = 270 mm, acquisition matrix = 270 $\times$ 218, and slice thickness = 3 mm) in the plane prescribed by the three-point planscan tool.

RCA vessel wall scan

The vessel wall MRI sequence mainly consisted of two parts: contrast generation, and image acquisition. Contrast between the RCA wall and the blood in the lumen was generated using the optimized local dual-inversion technique, which involves a non-selective inversion followed by the application of a cylindrical 2D selective local re-inversion of the magnetization in parallel to the main axis of the RCA.[5,6] We applied a 2D selective higher order local inversion pulse with a diameter of 5 cm and a total pulse duration of 8.2 ms in all subjects. Localization of the spatially selective magnetization preparation pulse was performed on the earlier described angiogram. The local inversion pre-pulse was placed to encompass the aortic cusp, ostium of the RCA, and the remainder of the vessel, ensuring that the blood-pool magnetization in the left ventricle was not re-inverted.

The RCA vessel wall was imaged in the plane defined by the three-point planscan tool. Imaging was performed in every other R–R interval using a spiral sequence with the following parameters: TR = 29 ms, TE = 2.3 ms, acquisition window = 59 ms, 20 slices, FOV = 400 mm, acquisition matrix = 512 $\times$ 512, and spatial resolution of 0.78 $\times$ 0.78 $\times$ 2 mm^3. The total number of cardiac cycles from which data were used to generate a complete 3D image was 252. The total scanning duration depends on both the heart-rate of the subjects and the individual navigator efficiency. The heart-rate dependent time-delay between the local inversion contrast enhancement pre-pulse and the imaging sequence was adjusted for maximized blood-signal suppression[11] and ranged from 550 to 650 ms.

Image analysis

The analysis was performed along the entire visualized course of the RCA using a previously reported semi-automatic edge detection 'soapbubble' tool, which measures dimensions.[12] To minimize digitization errors and to facilitate data analysis, the images were zoomed by a factor of four, using Fourier zooming.[13] We visually identified points on the coronary vessel wall per interactive mouse click, thus generating two sets of wall thickness values, for the anterior and the posterior vessel walls (*Figure 1*). The visible continuous length of the coronary vessel wall was measured manually. Subsequently, along the trace defined by the aforementioned user-defined points, a local image gradient was obtained utilizing a Deriche algorithm (where an edge image using a first-order derivative of the input image is generated), and wall thickness was automatically measured perpendicular to the vessel wall (distance between maximum image gradients perpendicular to the course of the vessel wall), in equidistant steps of 0.2 mm, as reported earlier.[14] For the visual inspection of the adequacy of the algorithm to measure the vessel wall thickness, the computer-identified inner (luminal) and outer (adventitial) boundaries of each vessel wall were graphically highlighted and overlaid on the anatomical image. If the automated measurement was visually identified as 'inadequate' by the operator, manual interaction and correction was performed. On the basis of our prior experience, this was primarily needed in the regions of branching vessels where the user could simply tell the algorithm to interrupt the measurements in the region of the branch to avoid bias. To ensure that the wall thickness measurements were performed at the same anatomical

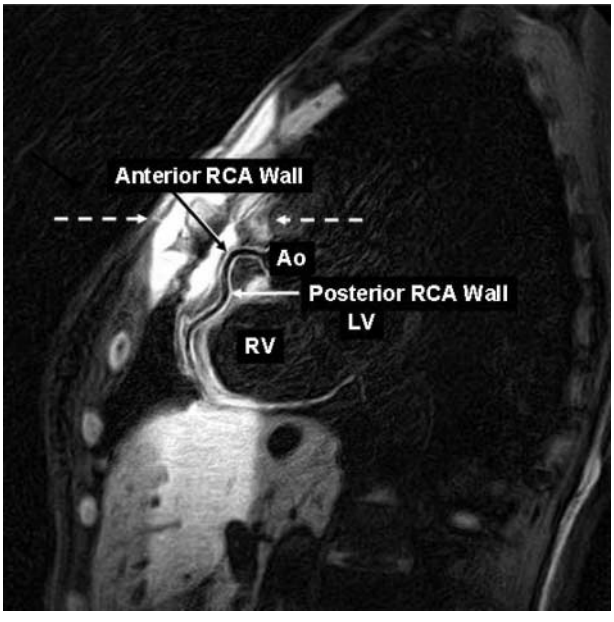

Figure 1 3D black-blood RCA vessel wall image showing the anterior and the posterior walls (arrows).The broken arrows point to the contrast between the tissue in the path of the cylindrical pulse and the surrounding tissue by use of the local inversion prepulse.

levels, Reader 1 (M.Y.D.) reported to Reader 2 (M.S.) the distance in millimetres from the RCA ostium where the semi-automated wall thickness measurements began and for what segment length (also in millimetres) the analysis was performed. For the measurement of vessel wall thickness on repeat scans, Reader 1 communicated to himself in a manner similar to that mentioned earlier.

Signal to noise ratio and contrast to noise ratio

Signal to noise ratio (SNR)/contrast to noise ratio (CNR) of the vessel wall scans were calculated on the raw image data, in a blinded manner, with the 'soapbubble' tool using the following formulae.

$$\mathrm{SNR} = \frac{\text{Signal intensity}_{\text{wall}}}{\text{Standard deviation}_{\text{background}}}$$

$$\mathrm{CNR} = \frac{\text{Signal intensity}_{\text{wall}} - \text{Signal intensity}_{\text{lumen}}}{\text{Standard deviation}_{\text{background}}}.$$

The regions of interests were manually traced over an extended length of the vessel wall, its adjacent lumen, and in the background anterior to the chest.

Statistical analysis

Continuous variables are reported as mean $\pm$SD. Paired *t*-testing (two-sided) was used to compare the continuous variables. After multiplanar reformatting by Reader 1 (M.Y.D.), two measurements (anterior and posterior wall thickness, *Figure 2*) were recorded in each individual. Subsequently, Reader 2 (M.S.) repeated vessel wall thickness measurements on these reformats. For intra-observer measurement, Reader 1 repeated the multiplanar reformatting and the measurements 1 week later in a blinded fashion. The same measurements were repeated by Reader 1 in eight volunteers who were re-imaged. On the basis of these measurements, intra-observer (two times Reader 1 measurements), inter-observer (Reader 1 vs. Reader 2 measurements), and inter-scan agreements (original Reader 1 vs. repeat Reader 1 measurements) were assessed using Pearson's correlation coefficient (*r*), Bland–Altman analysis,[15] and intra-class correlation coefficients.[16,17] Intra-class correlation coefficient is the proportion of total variability accounted for by the variability among readers. If the coefficient is high, it means only a small portion of the variability is due to variability in measurement on different occasions; hence, the reproducibility is high. The following formula was used to calculate the intra-class correlation coefficients: {(Variance$_{\text{measurement 1}}$ + Variance$_{\text{measurement 2}}$ − Difference in variance between measurements 1 and 2)/[(Variance$_{\text{measurement 1}}$ + Variance$_{\text{measurement 2}}$) + (Difference in the mean values of measurements 1 and 2)^2 − (Difference in variance between measurements 1 and 2/Total number of measurements)]}. Generalized estimating equations (GEE) were used to adjust standard errors (SE) for the clustering of two observations (anterior and posterior wall) within the same individual.[18] A *P*-value <0.05 was considered statistically significant.

Results

Vessel wall dimensions and reproducibility

All subjects completed the scans. The average age of the study cohort was 32 ± 6 years (range 25–43 years) and there were six women. The average heart-rate during image acquisition was 67 ± 12 b. p.m. (range 48–90). The average scanning time per 3D vessel wall scan was $\sim$12 min. With the 3D vessel wall imaging sequence, we were able to visualize an average of 44 ± 7 mm of the proximal RCA vessel wall and use it for quantitative analysis of the wall thickness. The average SNR and CNR were 16 ± 7 and 10 ± 6, respectively. The coronary vessel wall appeared distinct from the surrounding epicardial fat and the coronary blood pool. The 2D local dual inversion pulse effectively suppressed unwanted signals outside the region of interest. There was a sharp demarcation between the tissue in the path of the local inversion pre-pulse and the surrounding tissue (*Figures 1 and 2*). The outer walls of two subjects could not be analysed by one of the observers and hence were excluded from the analysis. In three subjects, both the walls were analysed manually, due to suboptimal identification of the vessel wall borders by the software.

The mean RCA vessel wall thickness was 1.6 ± 0.2 mm (1.7 ± 0.2 mm in men and 1.6 ± 0.2 mm in women). The

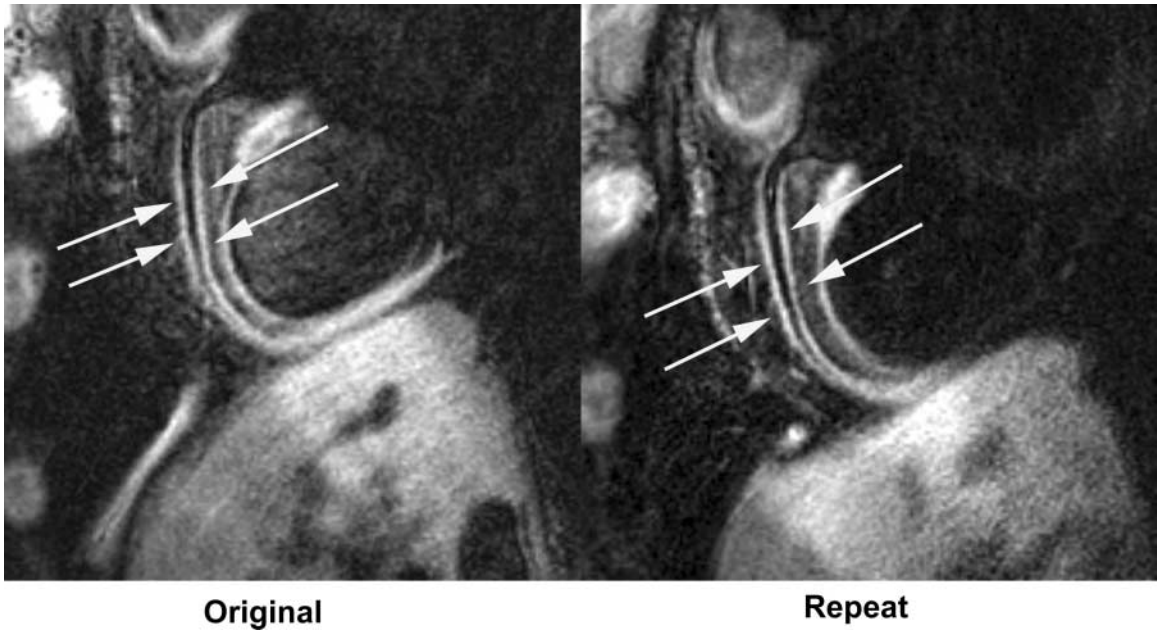

Figure 2 3D black-blood RCA vessel wall images, obtained $\sim$1 month apart, demonstrating excellent visual reproducibility.

mean vessel wall thickness (original and repeat values) for the subjects who underwent the scans twice measured 1.7 ± 0.2 and 1.7 ± 0.3 mm, respectively ($P = 0.48$).

Using Pearson's correlation coefficient, there was a highly statistically significant intra-observer ($r = 0.97$, $R^2 = 93\%$, SE = 0.06), inter-observer, ($r = 0.94$, $R^2 = 89\%$, SE = 0.08) and inter-scan ($r = 0.90$, $R^2 = 80\%$, SE = 0.12) concordance for semiautomatic vessel wall thickness measurements (all $P < 0.001$). The results of the Bland–Altman analysis demonstrating intra-observer, inter-observer, and inter-scan agreements are shown in *Figures 3 A, B, and C*. We found a high degree of intra-observer, inter-observer, and inter-scan concordance for vessel wall thickness measurements (intra-class correlation coefficients were 0.97, 0.92, and 0.86, respectively). GEE analysis also demonstrated significant association between Reader 1 and Reader 2 for intra-observer (regression estimate = 0.9630, SE = 0.03), inter-observer (regression estimate = 1.0117, SE = 0.05), and inter-scan (regression estimate = 0.9834, SE = 0.0925) analyses (all $P < 0.0001$).

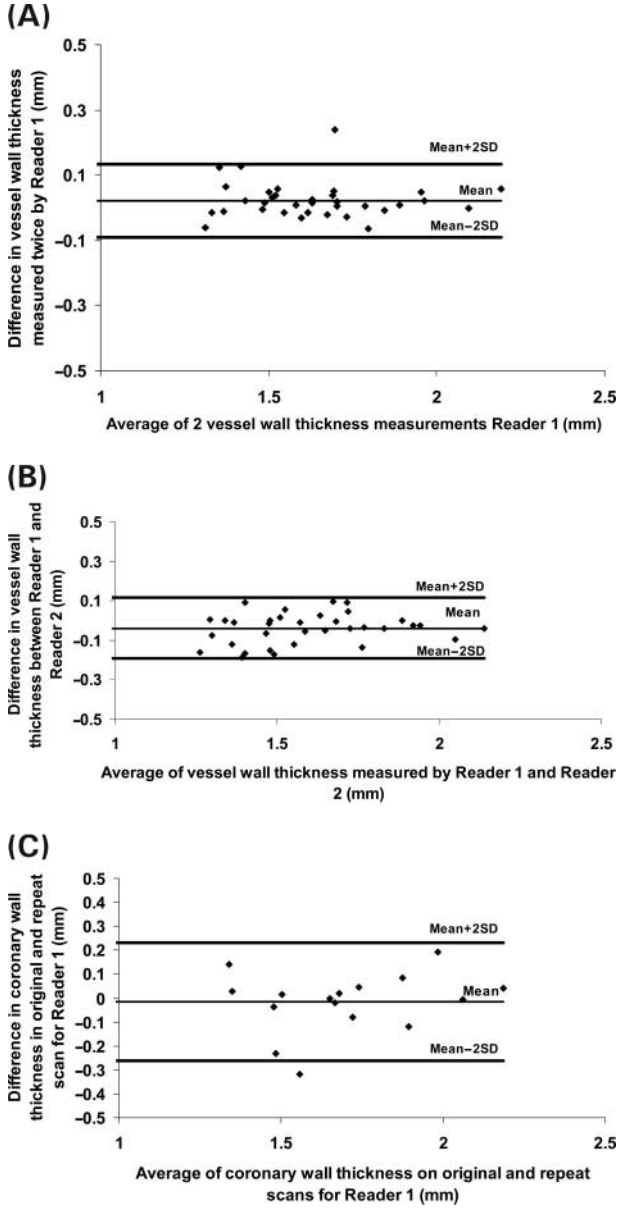

Figure 3 Bland–Altman graphs demonstrating the intra-observer (*A*), inter-observer (*B*), and inter-scan (*C*) concordance of coronary vessel wall thickness measurements obtained using the semi-automatic analysis 'soapbubble' tool.

Discussion

Reproducibility

This study demonstrates that the non-invasive magnetic resonance technique of 3D free-breathing black-blood coronary vessel wall imaging is feasible and highly reproducible (*Figures 2 and 3*). Utilizing a semiautomatic edge detection technique, we are able to demonstrate a very high degree of concordance (*Figure 3*) in repeat measurements of human coronary artery wall thickness, averaged over a long continuous segment of the RCA.

Improved contrast generation for vessel wall MR imaging

The 2D selective local inversion pre-pulse used in our study was a highly spatially selective cylindrical 2D local dual inversion pre-pulse, which lead to optimal suppression of the blood entering the coronary artery. This could potentially aid in maximizing the SNR in the region of the coronary vessel wall and avoid the in-flow of re-inverted blood pool magnetization into the coronary artery leading to an improved CNR.

Limitations

Although lacking a true *in vivo* gold-standard for comparison (e.g. IVUS), vessel wall thickness may be overestimated by this technique, when compared with previously published pathology reports.[19–21] This is most likely attributed to the partial volume effects, curvature of the vessel, residual myocardial motion, and stagnant flow at the blood-vessel border. The partial volume effect, which results from a relatively low spatial resolution, was likely the major contributing factor to the overestimation of the vessel wall thickness in the present study. Higher-field magnetic resonance systems may offer a means to increase the spatial resolution but their utility for coronary vessel wall imaging remains to be investigated more thoroughly. The slow flowing blood at the edge of the artery can also theoretically contribute to the overestimation of the wall thickness, but studies in carotid arteries suggest that this may not be a major factor.[22] Thus, although this non-invasive technique appears to be very reproducible, the precision in terms of true dimension assessment requires further testing and comparison with invasive measures of coronary wall thickness.

This technique, like many other cardiac MR applications, is dependent upon a stable heart-rate and is adversely affected by arrhythmias as data for each 3D volume set is acquired over multiple heart beats. The use of arrhythmia rejection software, that is becoming available on most modern MR systems, can potentially help to solve the problem. Finally, the results obtained in the RCA may not be directly extrapolated to other coronary vessels. On one hand, it is possible that the findings in the left coronary system might not be as robust as those from the RCA,

because of its increased relative distance from the surface coil, which may affect SNR and CNR. On the other hand, the reduced motion of the left coronary system could lessen motion-related artifacts.

Future outlook

Because of its non-invasiveness and high reproducibility, 3D black-blood MR vessel wall imaging may potentially serve as an excellent tool to study subclinical atherosclerosis and it appears to be well-suited for follow-up studies after intervention or as a tool to follow-up plaque regression after therapy.[23,24] On the basis of our results, in order to detect a 10% change in vessel wall thickness with an 80% power at the alpha level of 0.05, a future study would require a sample size of approximately 15 subjects (paired analysis). If the intention were to detect a 5% change, the sample size would be roughly 52 subjects. Improvements of this technique in terms of using higher magnetic field strengths and advanced molecular compounds may aid in the characterization of the changes in the coronary vessel wall, similar to other vascular beds.[25–27] Doing so might also have implications for managing patients with established coronary heart disease.

Conclusion

This study demonstrates that 3D free-breathing black-blood coronary vessel wall imaging is a highly reproducible non-invasive technique for the assessment of coronary vessel wall thickness. This method could potentially play a major role in future studies involving longitudinal follow-up of coronary plaque progression and follow-up after intervention. Further studies in subjects with known atherosclerosis are warranted.

Acknowledgements

This work was supported by a Biomedical Engineering Grant from the Whitaker Foundation (RG-02-0745), a grant from the Donald W. Reynolds Foundation, and by the NIH grant HL61912. Dr Stuber is compensated as a consultant by Philips Medical Systems NL, the manufacturer of equipment described in this presentation. The terms of this arrangement have been approved by the Johns Hopkins University in accordance with its conflict of interest policies.

References

1. Glagov S, Weisenberg E, Zarins CK, Stankunavicius R, Kolettis GJ. Compensatory enlargement of human atherosclerotic coronary arteries. *N Engl J Med* 1987;**316**:1371–1375.
2. Rumberger JA, Brundage BH, Rader DJ, Kondos G. Electron beam computed tomographic coronary calcium scanning: a review and guidelines for use in asymptomatic persons. *Mayo Clin Proc* 1999;**74**:243–252.
3. Nissen SE, Yock P. Intravascular ultrasound: novel pathophysiological insights and current clinical applications. *Circulation* 2001;**103**:604–616.
4. Fayad ZA, Fuster V, Fallon JT, Jayasundera T, Worthley SG, Helft G, Aguinaldo JG, Badimon JJ, Sharma SK. Noninvasive in vivo human coronary artery lumen and wall imaging using black-blood magnetic resonance imaging. *Circulation* 2000;**102**:506–510.
5. Kim WY, Stuber M, Bornert P, Kissinger KV, Manning WJ, Botnar RM. Three-dimensional black-blood cardiac magnetic resonance coronary vessel wall imaging detects positive arterial remodeling in patients with nonsignificant coronary artery disease. *Circulation* 2002;**106**:296–209.
6. Botnar RM, Kim WY, Bornert P, Stuber M, Spuentrup E, Manning WJ. 3D coronary vessel wall imaging utilizing a local inversion technique with spiral image acquisition. *Magn Reson Med* 2001;**46**:848–854.
7. Fischer SE, Wickline SA, Lorenz CH. Novel real-time R-wave detection algorithm based on the vectorcardiogram for accurate gated magnetic resonance acquisitions. *Magn Reson Med* 1999;**42**:361–370.
8. Danias PG, McConnell MV, Khasgiwala VC, Chuang ML, Edelman RR, Manning WJ. Prospective navigator correction of image position for coronary MR angiography. *Radiology* 1997;**203**:733–736.
9. Wang Y, Riederer SJ, Ehman RL. Respiratory motion of the heart: kinematics and the implications for the spatial resolution in coronary imaging. *Magn Reson Med* 1995;**33**:713–719.
10. Stuber M, Botnar RM, Danias PG, Sodickson DK, Kissinger KV, van Cauteren M, De Becker J, Manning WJ. Double-oblique free-breathing high resolution three-dimensional coronary magnetic resonance angiography. *J Am Coll Cardiol* 1999;**34**:524–531.
11. Fleckenstein JL, Archer BT, Barker BA, Vaughan JT, Parkey RW, Peshock RM. Fast short-tau inversion-recovery MR imaging. *Radiology* 1991;**179**: 499–504.
12. Etienne A, Botnar RM, van Muiswinkel AM, Boesiger P, Manning WJ, Stuber M. 'Soap-Bubble' visualization and quantitative analysis of 3D coronary magnetic resonance angiograms. *Magn Reson Med* 2002;**48**: 658–666.
13. Parker DL, Du YP, Davis WL. The voxel sensitivity function in Fourier transform imaging: applications to magnetic resonance angiography. *Magn Reson Med* 1995;**33**:156–162.
14. Botnar RM, Stuber M, Danias PG, Kissinger KV, Manning WJ. Improved coronary artery definition with T2-weighted, free-breathing, three-dimensional coronary MRA. *Circulation* 1999;**99**:3139–3148.
15. Bland JM, Altman DG. Statistical methods for assessing agreement between two methods of clinical measurement. *Lancet* 1986;**1**:307–310.
16. Bartko JJ. The intraclass correlation coefficient as a measure of reliability. *Psychol Rep* 1966;**19**:3–11.
17. Deyo RA, Diehr P, Patrick DL. Reproducibility and responsiveness of health status measures. Statistics and strategies for evaluation. *Control Clin Trials* 1991;**12**:142S–158S.
18. Zeger SL, Liang KY, Albert PS. Models for longitudinal data: a generalized estimating equation approach. *Biometrics* 1988;**44**:1049–1060.
19. Velican D, Petrescu C, Velican C. Prevalence of the 'normal' aspect of the coronary arteries in an unselected population sample of Bucharest aged 1–60 years. *Med Interne* 1987;**25**:113–119.
20. Velican D, Velican C. Coronary anatomy and microarchitecture as related to coronary atherosclerotic involvement. *Med Interne* 1989;**27**:257–262.
21. Litovsky SH, Farb A, Burke AP, Rabin IY, Herderick EE, Cornhill JF, Smialek J, Virmani R. Effect of age, race, body surface area, heart weight and atherosclerosis on coronary artery dimensions in young males. *Atherosclerosis* 1996;**123**:243–250.
22. Melhem ER, Jara H, Yucel EK. Black blood MR angiography using multislab three-dimensional TI-weighted turbo spin-echo technique: imaging of intracranial circulation. *AJR Am J Roentgenol* 1997;**169**:1418–1420.
23. Nissen SE, Tsunoda T, Tuzcu EM, Schoenhagen P, Cooper CJ, Yasin M, Eaton GM, Lauer MA, Sheldon WS, Grines CL, Halpern S, Crowe T, Blankenship JC, Kerensky R. Effect of recombinant ApoA-I Milano on coronary atherosclerosis in patients with acute coronary syndromes: a randomized controlled trial. *JAMA* 2003;**290**:2292–2300.
24. Nissen SE, Tuzcu EM, Schoenhagen P, Brown BG, Ganz P, Vogel RA, Crowe T, Howard G, Cooper CJ, Brodie B, Grines CL, DeMaria AN. Effect of intensive compared with moderate lipid-lowering therapy on progression of coronary atherosclerosis: a randomized controlled trial. *JAMA* 2004;**291**:1071–1080.
25. Wasserman BA, Smith WI, Trout HH III, Cannon RO III, Balaban RS, Arai AE. Carotid artery atherosclerosis: in vivo morphologic characterization with gadolinium-enhanced double-oblique MR imaging initial results. *Radiology* 2002;**223**:566–573.
26. Yuan C, Kerwin WS, Ferguson MS, Polissar N, Zhang S, Cai J, Hatsukami TS. Contrast-enhanced high resolution MRI for atherosclerotic carotid artery tissue characterization. *J Magn Reson Imaging* 2002;**15**:62–67.
27. Winter PM, Caruthers SD, Yu X, Song SK, Chen J, Miller B, Bulte JW, Robertson JD, Gaffney PJ, Wickline SA, Lanza GM. Improved molecular imaging contrast agent for detection of human thrombus. *Magn Reson Med* 2003;**50**:411–416.